The Fifth International Symposium on Diagnostics and Modeling of Combustion in Internal Combustion Engines
(COMODIA 2001), July 1•4, 2001, Nagoya

(1-23) A Study of the Formation and Break-Up of a Diesel Spray for HSDI Diesel Engine Combustion Systems

R. Morgan, M. Gold, J.Wray and S. Whelan
Ricardo Consulting Engineers Ltd

ABSTRACT

The use of in-cylinder computational fluid dynamics (CFD) to model fuel and air interaction is increasingly being used to rapidly design and develop direct injection combustion systems. Use of such CFD techniques has substituted many physical engine testing experiments and hence shortened development times. However, the fundamental propagation of diesel fuel spray is critical in resolving air and fuel mixing characteristics. The lack of realistic measured diesel spray data and inappropriate phenomenological correlation lead the authors to investigate diesel fuel spray at conditions representative of a modern common rail equipped turbocharged and after-cooled HSDI diesel engine.

Operating conditions were achieved in an optical rapid compression machine fitted with a common rail fuel injector. The initial stages of these investigations are described within this paper, where both stills and high speed imaging techniques were used.

The influences of injector nozzle configuration, injection pressure and air charge conditions on the diesel fuel spray were examined using back-lighting techniques. Qualitative differences in spray structure were observed between tests performed with short and long injection periods. Changes in the flow structure within the nozzle could be the source of this effect. Differences in the fuel spray liquid core were observed between VCO (Valve Covers Orifice) and mini-sac nozzles, with the mini-sac nozzles showing a higher rate of penetration under the same conditions.

INTRODUCTION

Developments in engine simulation technology have made the 'virtual engine' model a realistic proposition [1]. The use of Computational Fluid Dynamics (CFD) on engine development programmes has enabled significant time and cost savings to be made in the design and development of the engine combustion system. Accurate modelling of the fuel spray formation and mixing process is a key part of a successful combustion simulation.

Several spray break up models have been proposed in recent years [2,3,4] and have yielded good results when implemented in commercial CFD codes [5]. Accurate simulation of the fuel spray formation process can be achieved by inputting measured data as a boundary condition into the simulation, such as spray cone angle and droplet distribution from calibration tests on the fuel system in question. However, a preferable approach is to be able to simulate the influence of the injector design on spray formation by inputting readily available geometric parameters alone into an empirical model or direct simulation of the internal flow within the injector. Either approach requires extensive validation to ensure the correct boundary conditions are derived across the expected operating range of the engine.

In order to check the validity of the fuel spray model, an extensive experimental programme has been undertaken by Ricardo to gather data on the spray formation and break-up process at conditions representative of modern and future diesel engines. A rig has been installed at the University of Brighton to enable research on the fuel spray to be performed using a modern common rail fuel system at conditions representative of those found in a diesel engine. The first phase of this work, reported in this paper, covers imaging work on the fuel spray over a wide range of test conditions. The influence of injection pressure and nozzle geometry on the behaviour of the fuel spray has been studied at a range of ambient pressure and temperature conditions. The results, in terms of the liquid penetration length and dispersion angle have been compared with a number of established empirical models.

EXPERIMENTAL APPARATUS

High Pressure Spray Rig

A high pressure and temperature spray and combustion research facility was installed in 1999 at The University of Brighton in the United Kingdom. The facility was designed to enable spray and combustion studies to be performed at conditions representative of a modern TCA diesel engine. The design of the new facility has been described in the past [20,21,22]. The main features are:

- Independent control of air pressure and density
- Air pressures in the range of 3 to 13 MPa
- Air temperatures in the range of 570 K to 1000 K
- Multiple consecutive injections of fuel
- Quiescent air motion during the injection and spray formation process

The rig is based on a reciprocating rapid compression machine with a large optical chamber into which the spray is introduced. The chamber is 50 mm in diameter and 70 mm long. Interaction with the wall would be expected to be minimal for a fuel spray of the type produced by an injector used in a passenger car engine. A schematic of the spray chamber is shown in Figure 1.

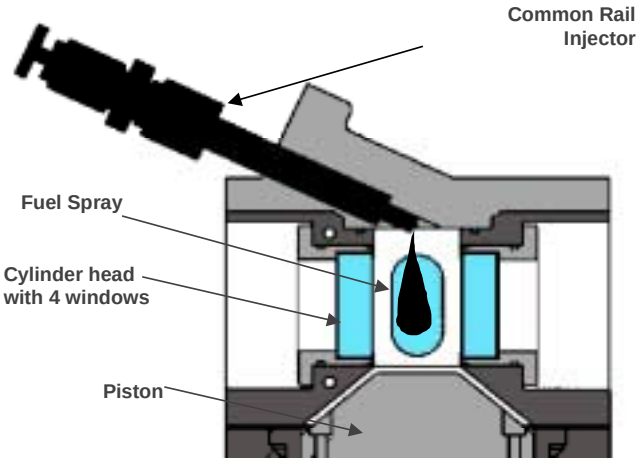

Figure 1 Schematic of the spray chamber

The air pressure and temperature at the start of injection are controlled by conditioning the charge air into the engine by means of an air compressor and heater. The inducted air is then compressed in the engine to the desired test conditions. CFD analysis has previously confirmed the air motion within the combustion chamber is essentially quiescent [21]. The maximum air velocity in the chamber during the injection process was predicted to be less than 1 m/s in the axial direction of the spray.

Fuel System

A second generation Bosch common rail system [23] was used for this work, with a maximum rail pressure capability of 160 MPa. The fuel pump was powered by an electric motor maintained at 1400 rev/min to ensure a stable rail pressure with minimal fluctuation. The fuel rail and delivery pipe were both instrumented with a 4067 Kistler pressure transducer. The pipe from the rail to the injector was minimised to represent that of a passenger car. A custom controller [21] was manufactured to enable independent control of injection timing, injection duration and rail pressure. Figure 2 illustrates and compares the injection rate profile delivered form our custom controller.

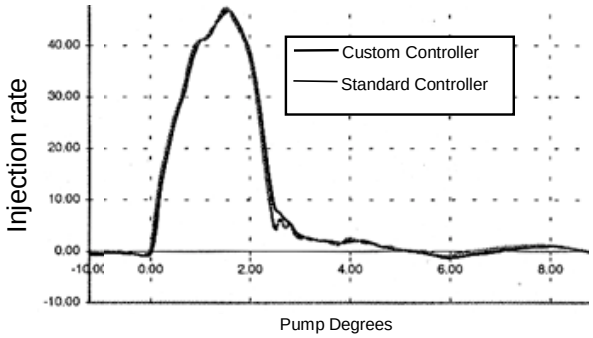

Figure 2 Injection rate diagram from standard and custom controller

A number of nozzles were used in this study, as summarised in Table 1.The nozzles were of a single-hole design with an equivalent spray angle of 130°. The holes were manufactured by a conventional spark erosion technique and then micro-honed to produce an entry radius and surface finish representative of a production nozzle. The needle was of the double guided type and was instrumented with a Hall effect type needle lift sensor. Previous work [14] has shown hole to hole variability due to poor concentricity of the needle within the VCO nozzle. Ambient pressure spray imaging, shown in Figure 3, of a single hole nozzle was performed and confirmed the general spray structure was representative of the multi-hole nozzle.

Nozzle Type	Orifice diameter (mm)	Lift / diameter (L/d)
VCO	0.10	10.0
VCO	0.15	6.8
VCO	0.20	5.0
Mini-sac	0.10	10.0
Mini-sac	0.15	6.8
Mini-sac	0.20	5.0

Table 1: Details of nozzles used in the study

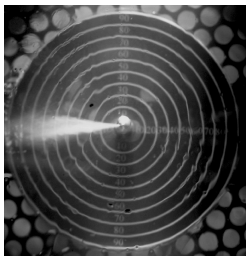

Figure 3 Single hole fuel spray under ambient conditions

Injector Calibration

The complete fuel system, including pump, rail, pipe-work and controller was calibrated on a Lucas rate gauge. A correlation between injection duration and injected fuel mass was establish by the calibration of each nozzle. Fuel flow was not measured during the imaging experiments but was derived from the injection duration and nozzle calibration. The same injector was used for the duration of these experiments. The injection rate was checked on the Lucas rate gauge after each nozzle change to confirm consistency of injector performance prior to testing on the spray rig.

EXPERIMENTAL TECHNIQUE

General Test Procedure

The spray rig was prepared for each test by pre-heating the cylinder head and liner to 80 ℃. In addition, the inlet pipe-work was pre-heated for the hot tests by flushing through with heated air. The air temperature and pressure at TDC were controlled by pre-conditioning the charge air to the desired temperature and pressure and compressing to the test conditions. The back pressure across the engine was set to maintain good scavenge efficiency and acceptable air flow. The cylinder pressure, fuel pressure and needle lift were captured on a digital storage scope and system temperatures and pressures on a low speed data logger. The low-sulphur diesel used for all the tests had the following properties:

- Density 840 kg/m^3
- Cetane Number 51
- Sulphur Content < 0.03%

In the work presented a number of injection strategies were considered covering representative fuelling quantities from pilot through to heavy load conditions, as shown in Table 2. The total amount of fuel injected was calculated from the injection duration.

Injection pressure (MPa)	Orifice diameter (mm)		
	0.2	0.15	0.1
60	Fuelling quantities from 3 to 50 mm^3		
100			
140			
160			

Table 2: Fuel injection conditions studied

Image acquisition

High resolution imaging was performed with a fully manual Pentax SLR camera incorporating a telephoto lens (125 mm, f:1/4-1/22) and two extension tubes (1+3 cm). This combination was found to give the best compromise between magnification and focal distance. The acquired back lit images provide an area-integrated image of the fuel spray. High speed imaging was performed with a CCD video camera. The model used in this series of experiments was a Kodak Ektapro HS Motion Analyzer (Model 4540). The best compromise between acquisition rate and image resolution was obtained with a frame rate of 18000 pictures per second, with a corresponding resolution of 256×64 pixels × 256 levels of grey.

Image Processing

A typical unprocessed image is shown in Figure 4a, the spray nozzle tip is located 20 mm to the right of the window edge and is therefore not visible. The spatial resolution was calculated to be 0.36 mm per pixel.

The use of a threshold value was employed to outline the spray from the background. The threshold level was manually chosen by selecting one image from the batch of images generated by a test run and varying the threshold to obtain optimum results. Since the image illumination was constant during a test run, this threshold value was suitable for all the images in that batch. Figure 4a and 4b show raw and thresholded images.

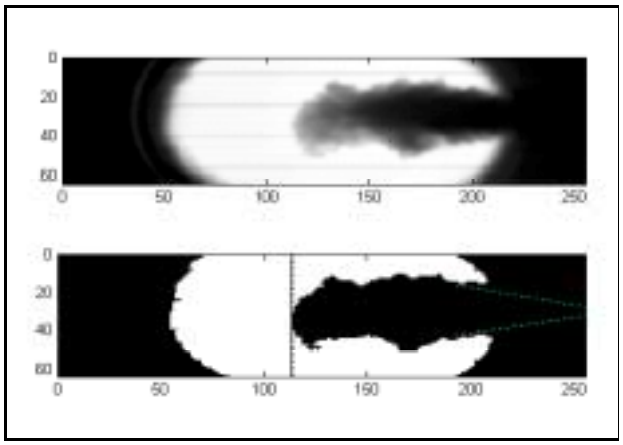

Figure 4 (a) Raw digital spray image; 4(b) Thresholded image showing maximum penetration length

The spray data was measured in two ways; firstly the maximum spray penetration was calculated by finding the spray pixel furthest from the nozzle. This value of penetration was then used to calculate the spray angle at half the maximum penetration length.

Once the spray angle was known the refined spray penetration was calculated using a second method, described by Naber and Siebers [9]; this defines spray penetration as "the distance along the spray axis to a location where ½ of the pixels on an arc of θ/2 centred on the spray axis are dark", this definition was simplified for computational reasons and a straight line was used instead of an arc as shown in Figure 5. This modification was found to have a negligible effect on the calculated values of penetration, when compared with the method described by Naber and Siebers [9].

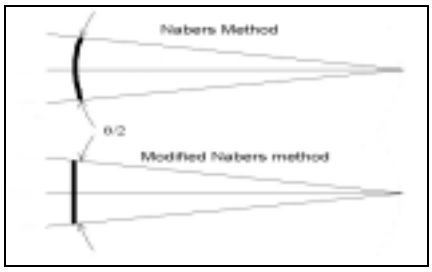

Figure 5 Definition of spray penetration length

By initialising with the maximum penetration value to calculate the spray angle, the iterative approach used by Naber and Siebers [9] was avoided. In most cases there was very little difference between the maximum penetration and the penetration calculated using the modified Naber and Siebers [9] criteria.

RESULTS AND DISCUSSION

Preliminary laser sheet imaging [20] identified a number of areas of interest for high-resolution photography. Photographic tests were performed at:

- Fuel pressures between 60 and 160 MPa
- Ambient air pressures between 3 and 8 MPa
- Ambient air temperature of 540K
- Injection duration from 0.9 to 3.41 ms
- Single-hole VCO nozzle with 0.2mm diameter

A sequence of images taken 1ms after the start of injection for a 3.41ms injection is shown in Figure 6. The images were taken at two values of ambient pressure and four values of rail pressure at an ambient temperature of 540K. The spray can be considered essentially non-evaporating at this temperature. The expected increase in penetration resulting from an increase in injection pressure or decrease in air pressure is observed. The structure of the spray is consistent with previous observations [24, 25], with areas of atomised droplets being entrained at the edge of the spray where fuel air interaction takes place. The influence of air density can be seen between Figures 6a and 6b, with the higher air density resulting in a reduction in spray tip penetration, particularly for the lower injection pressures.

During initial stages of injection a concentrated "bunching" of spray at the leading edge of the jet is formed as droplets penetrate the stagnant gas field, re-circulating areas of droplets are observed to "peel" back along the edge of the spray cone from this area. This droplet stripping process was observed for all injection conditions and is depicted in the sequence in Figure 7 (negative images have been used to increase clarity). The formation of a head vortex due to the entrainment of dense air can be seen more clearly at the higher air density cases.

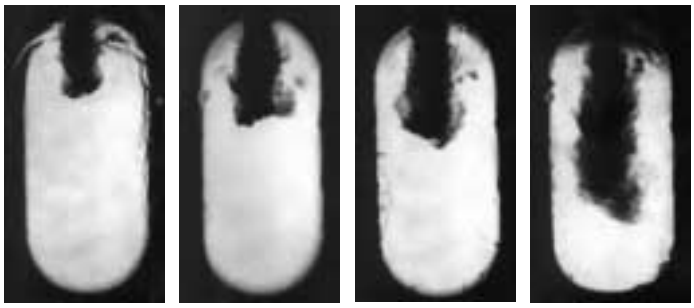

60 MPa 100 MPa 130 MPa 160 MPa

Figure 6 (a) Back lit spray images taken 1 ms after the start of injection in air at 3 MPa with an injection duration of 3.41 ms at four fuel rail pressures

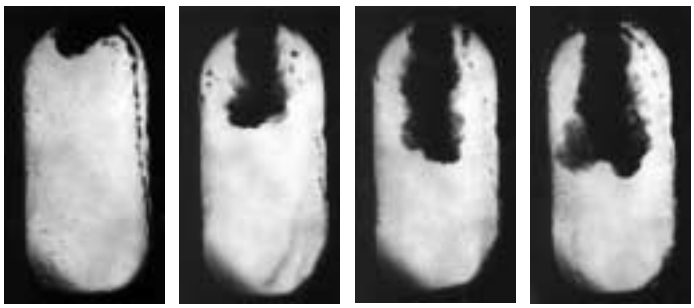

60 Mpa 100 MPa 130 MPa 160 MPa

Figure 6 (b) Back lit spray images taken 1 ms after the start of injection in air at 8 MPa with an injection duration of 3.41 ms at four fuel rail pressures

A similar sequence of images is shown in Figure 8a and 8b for a 0.9 ms injection duration. The spray structure is observed to be slightly different when compared with the 3.41 ms injection case. In the 0.9ms period case, the injector needle will only briefly achieve full lift, resulting in a throttling of the fuel flow under these conditions. Fuel is therefore predominantly injected during throttling, hence the orifice internal flow structure would be expected to be different to that of the 3.41 ms case. This effect has been observed in steady state large scale nozzle tests [14] particularly with VCO nozzles. It demonstrates the importance of understanding the effect of internal orifice flow structure on the behavior of spray.

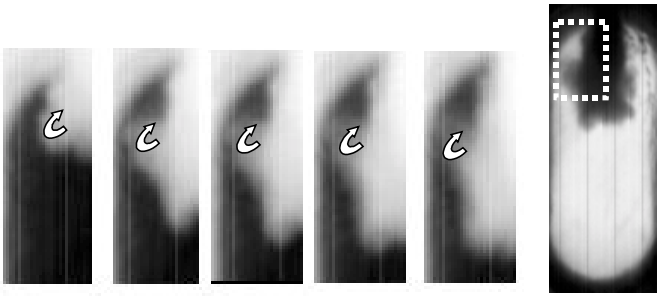

Figure 7 Development of areas of droplets "peeling" back along the spray plume. Enlarged images presented are from 1.1ms ASOI to 1.4 ms ASOI.

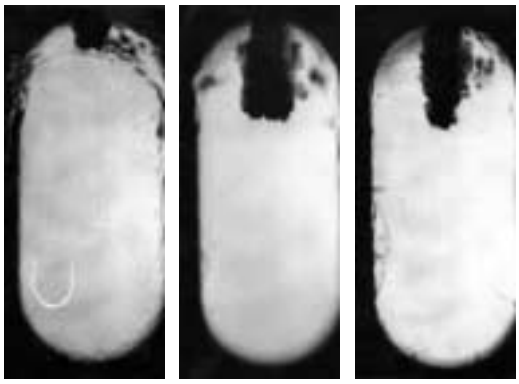

60 MPa 100 MPa 130 MPa

Figure 8 (a) Back lit spray images taken 0.9 ms after the start of injection in air at 3 MPa with an injection duration of 0.9 ms at three fuel rail pressures

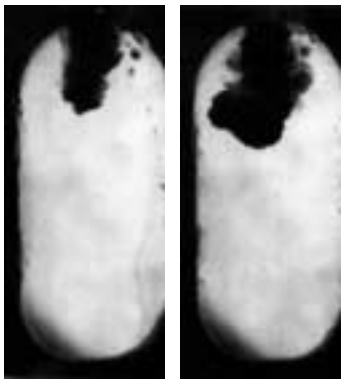

100 MPa 130 MPa

Figure 8 (b) Back lit spray images taken 0.9 ms after the start of injection in air at 8 MPa with an injection duration of 0.9 ms at two fuel rail pressures

Influence Of Fuel Pressure

Figure 9 shows the effects of increasing fuel rail pressure on a VCO (0.2mm) nozzle spray.

As expected, higher rail pressures result in a higher rate of spray tip penetration. It was however found that there was little difference between 160 and 130 MPa rail pressure results. Spray penetration is generally reported to be a function of the pressure difference across the nozzle:

$$S \propto (\Delta P)^{0.25}$$

According to this relationship, the effect on penetration of a change in injection pressure would be reduced at higher injection pressures. Similarly injector body and nozzle throttling and hence pressure loss becomes more significant for increasing fuel rail pressures. These features could explain the observed result. In addition, it has been previously reported that higher injection pressures result in an increase in the atomisation rate of the spray and result in a decrease in the mean liquid droplet size [26]. It would be expected that the smaller droplets would evaporate at a higher rate, resulting in a reduction in the liquid core length of the spray. The imaging technique used in this work will only detect liquid fuel and so evaporation (and very small droplets) will influence the ultimate visible liquid penetration length. Schlieren photography will be used to test this hypothesis in the next testing phase.

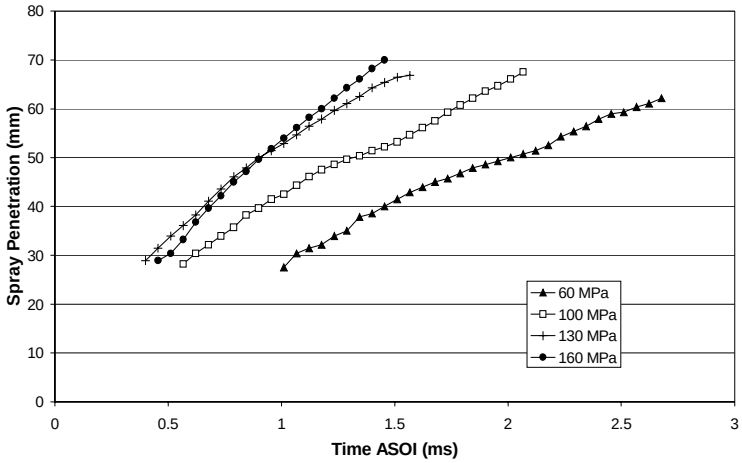

Figure 9 Comparison of experimental penetration rate for varying fuel rail pressures (0.2 mm VCO)

Influence Of Nozzle Type

Two nozzle designs and three nozzle geometries were tested. The main dimensions are summarised in Table 1. Figure 10 shows a comparison of penetration rate at one operating condition (in-cylinder pressure = 12Mpa; rail pressure = 100Mpa). The fuelling amount per injection was maintained constant throughout by changing the injection period.

A higher penetration rate is observed for the larger nozzle orifice diameters and for the mini-sac compared to VCO nozzle. The smaller diameter orifice would be expected to improve nozzle derived atomisation, hence the spray would contain smaller droplets. Again, the higher evaporation rate of these smaller droplets could explain the observed result. The observed difference between the two nozzle designs is interesting. None of the empirical models considered account for geometry effects upstream of the orifice which is the only difference between these two configurations. Previous work by Heimgärtner and Leipertz [28] has reported the mean droplet size from a VCO nozzle can be up to 50% smaller than the equivalent mini-sac nozzle. Again, this would result in a higher rate of evaporation and could explain the observed result. It has also been shown that VCO nozzle injectors cause a greater pressure loss within the nozzle geometry hence a lower 'Δp' at the nozzle orifice and lower spray penetration. These results emphasises the importance of understanding the influence of nozzle and injector geometry on fuel sprays.

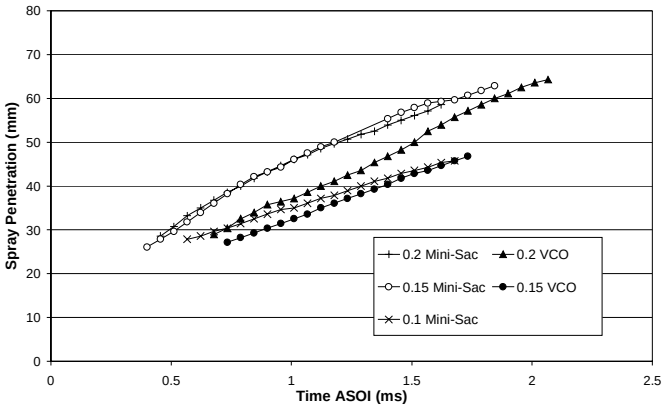

Figure 10 Comparison of experimental penetration rate for varying nozzle sizes and types

Influence Of Air Temperature

Tests were carried out under two temperature conditions. The intake air was heated such that the in-cylinder temperature at "top dead centre"(TDC) was either 577K or 701K. Evaporation will occur at both test conditions, but at a much slower rate at 577K. The increase in air temperature between the two conditions will also result in a decrease in air density of around 14 kg/m^3. The models considered predict that a rise in temperature should cause the spray penetration rate to increase due to the lower air density as illustrated by the Naber and Siebers [9] model predictions in Figure 11.

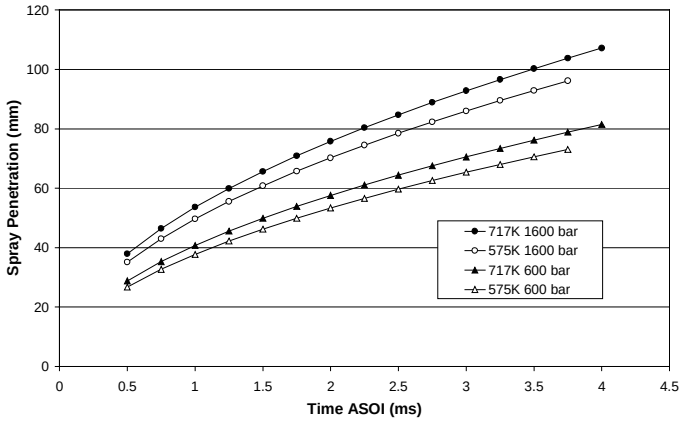

Figure 11 Naber and Siebers [9] model predictions showing the effect of in-cylinder temperature on spray penetration for two different pressures (0.2 mm nozzle)

The range of data used to investigate the model presented by Naber and Siebers [9] was gathered over a wide range of ambient air densities, temperatures, injection pressures and nozzle diameters. The range of injection pressures and ambient air densities for the present work and that used in the experiments of Naber and Siebers [9] are presented in Figure 12. The injection nozzle parameters and ambient temperature conditions are presented in Table 3. The injection profile used in the work of Naber and Siebers [9] used a non-rate shaped top hat profile unlike that presented in the current work, see figure 2. These injection rate differences should be appreciated when comparing the data sets from both experiments, especially when considering low fuelling when the injector needle will only partially achieve full lift.

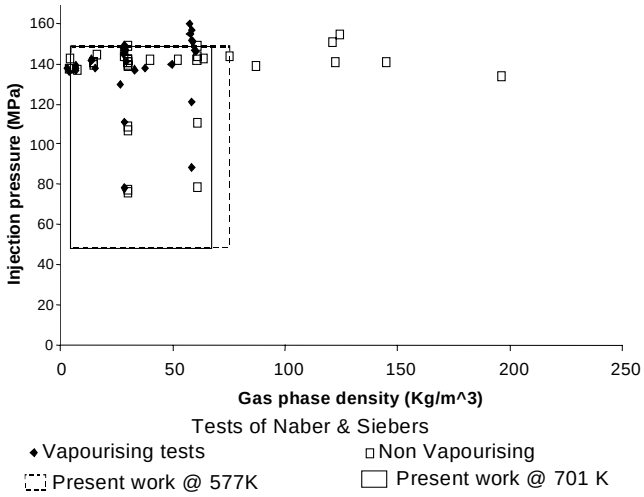

Figure 12 Comparison of range of injection conditions for the present work and that of Naber and Siebers [9] used to develop their penetration model.

	Naber and Siebers	Present work
Nozzle type	Mini-sac	VCO and Mini-sac
Orifice diameter (mm)	0.198 -0.340	0.1 -0.2
Orifice off-axis angle (°)	34	65
Gas phase temperature (K)	300 -452, non-evaporating spray	507
	607 -1405, evaporating spray	701

Table 3 Injection conditions and nozzle types used

According to Naber and Siebers [9] the changing effect of ambient temperature on the spray penetration was negligible in the range of 600-1400K and conditions of high density, representative of the settings presented in the current work (density > 28.6 kg/m^3). As shown in Figure 12, the penetration rate was found to be similar at 60 MPa rail pressure for the two test temperatures, supporting Naber and Siebers' higher density conclusion. The stable penetration length is observed to be significantly shorter for the higher temperature case as would be expected due to the higher evaporation rate.

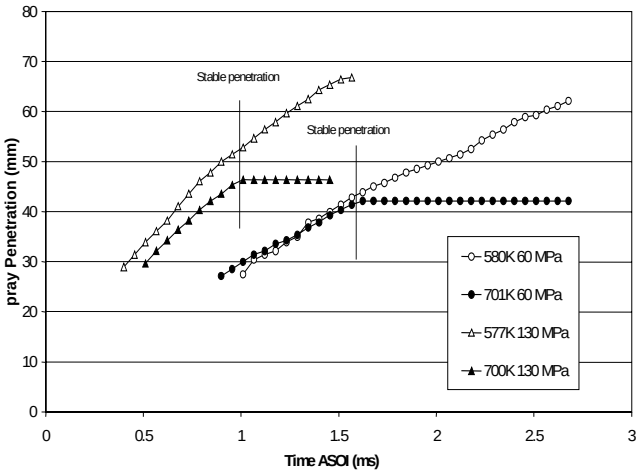

Figure 12 Experimental data showing the effect of in-cylinder temperature on spray penetration for two injection pressures, 60 and 130 MPa

The experimental results (Figure 12) do not however support the observation of Naber and Siebers [9] in the case of higher injection pressure. The higher injection pressure case shows a reduction in penetration rate with increasing temperature, despite the reduction in air density. This can be explained since for the higher injection pressure, the rate at which fuel enters the chamber is raised[1], increasing the spray cooling effect and creating a local rise in ambient density around the penetrating spray. Subsequent injected fuel has to penetrate this denser environment, leading to a reduction in spray penetration.

In both high temperature cases the ultimate spray length is observed to be similar i.e. independent of injection pressure. The stable core length at 130 MPa is however achieved more rapidly than in the 60 MPa case. All sprays injected into higher temperature environments were observed to reach a stable penetration length and maintain this level of the penetration until the end of the injection period. Similar effects have been observed by others investigating evaporating sprays [28].

Of the current models considered [9,15,16,17], only Dent [15] includes a term to compensate for evaporation:

$$S \propto \left(\frac{294}{T_a} \right)^{0.25}$$

This term however does not compensate enough to predict the results shown in Figure 16. The model predicts a 5% change in penetration whereas a 13-18% change is observed. Although some of the disparity may be attributed to different initial injection conditions (nozzle type, off axis angle etc.), further work is required if the influence of evaporation is to be effectively modelled in a simple empirical relationship.

[1] The injection period is reduced to maintain the fuelling amount constant

A direct comparison of experimental penetration measurements with predictions from the model presented by Naber and Siebers [9] are presented In Figure 13. Under these conditions the model over-predicts penetration when compared to both the low and high temperature experimental cases, although there is some agreement for the penetration of the low temperature case in the later stages of injection. These differences again may be attributed to differences in nozzle geometries and injection rate shapes between this work and the experiments used in deriving the relationships. Caution should be applied when predicting penetration from such relationships, it is evident that the temperature effect of reducing liquid penetration to a stable constant length is not predicted by any of the reviewed models, subsequently application of these models may lead to substantial over prediction of spray penetration.

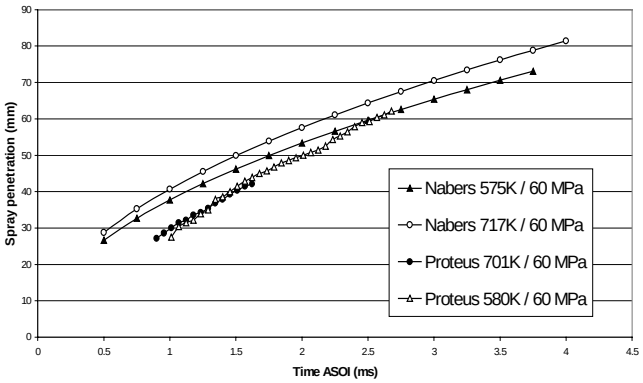

Figure 13 Comparison of experimental and predicted penetration

CONCLUSIONS

The influences of nozzle tip geometry, ambient pressure and temperature and fuel pressure were studied over a range of conditions representative of a modern diesel engine. Significant differences in spray structure were observed between long and short injection periods. This could be due to differences in internal flow structure within the nozzle at low needle lift.

The expected trends with injection pressure were observed. At higher injection pressure a lower rate of penetration than expected was observed, where the effect on penetration of a change in injection pressure is reduced at these higher injection pressures. In addition, the increased rate of evaporation at high injection pressures may also influence the penetration rate of the spray.

The VCO nozzles were observed to show a lower rate of penetration than mini-sac nozzles of the same dimensions. It is proposed that this is due to improved atomisation of the spray from the VCO nozzle, possibly due to differences in internal flow structure, resulting in a higher rate of evaporation.

Temperature was observed to influence the rate of liquid penetration when maintaining a constant ambient pressure. The effect was most pronounced at high injection pressures where the mean droplet size would be expected to be small. The rate of injection was also shown to have an effect on the local cooling of the gas adjacent to the penetrating spray, causing a retardation of the vaporising sprays at higher fuelling rates. This effect, coupled with faster evaporation of the smaller droplets which are produced at higher injection pressures, is suggested as the cause of the apparent reduction in spray tip penetrations. Further investigation is planned in this area.

Caution should be exercised when applying models to predict spray penetration and particular attention should be focused on the injection conditions and nozzle geometry. In the current work, it was found that the effect of injecting into high temperature conditions was to shorten penetration and that penetration length stabilised after a certain injection duration. This effect was not captured in the existing penetration models studied.

ACKNOWLEDGMENTS

The authors would like to thank mr, Kennaird, Mr, Crua, Mr Wood and Mr Whitney of The University of Brighton and Mr West at Ricardo for their assistance in gathering the data used in this paper. Thanks must also go to the EPSRC, UK for the loan of the high-speed camera equipment. We would also like to thank the directors of Ricardo for allowing the publication of this paper.

REFERENCES

1. G. Li, S.M. Sapsford and R.E. Morgan. CFD Simulation of a DI Truck Diesel Engine Using Vectis. SAE2000-01-2940
2. M.A. Patterson and R.D. Reitz. Modeling the Effect of Fuel Spray Characteristics on Diesel Engine Combustion and Emissions. SAE980131
3. R.D. Reitz and R. Diwakar. Effect of Drop Breakup on Fuel Sprays. SAE860469
4. A.B. Liu, D. Mather and R.D. Reitz. Modeling the Effects of Drop Drag and Breakup on Fuel Sprays. SAE980073
5. C. von Kuensberg Sarre, S.-C. Kong and R.D. Reitz. Modelling the Effects of Injector Nozzle Geometry on Diesel Sprays. SAE1999-01-0912
6. P.L. Herzog. Fuel Injection The Key to Effective Low-Emission Diesel Engines. IMechE S492/K1/99
7. N.S. Jackson. The High Speed Direct Injection Diesel Engine - Future Potential. THIESEL 2000, Valencia 13-15 September 2000.
8. A. Ilyama, Y. Matsumoto, K. Kawamoto, T. Ohishi. Spray Formation Improvement of VCO Nozzle for DI Diesel Smoke Reduction. IMechE Conference on Diesel Fuel Injection Systems 1992.
9. J. Naber and D.L. Siebers. Effects of Gas Density and Vaporization on Penetration and Dispersion of Diesel Sprays. SAE960034
10. D. Potz, W. Christ and B. Dittus. Diesel Nozzle-The Determining Interface Between Injection System and Combustion Chamber. THIESEL 2000, Valencia 13-15 September 2000.
11. C.H. Bae and J. Kang. Diesel Spray Characteristics of Common-Rail VCO Nozzle Injector. THIESEL 2000, Valencia 13-15 September 2000.
12. C. Arcoumanis and J. Whitelaw. Is Cavitation Important in Diesel Engine Injectors? THIESEL 2000, Valencia 13-15 September 2000.
13. C. Soteriou, R. Andrews and M. Smith. Diesel Injection –Laser Light Sheet Illumination of the Development of Cavitation in Orifices. Combustion Engines and Hybrid Vehicles, London, 28-30 April 1998, I.Mech.E., Paper C529/018/98
14. C. Soteriou and R. Andrews. Cavitation Hydraulic Flip and the Atomization in Direct Injection Diesel Sprays. IMechE C465/051/93
15. H. Hiroyasu and M. Arai. Structures of Fuel Sprays in Diesel Engines. SAE900475
16. J.C. Dent. A Basic Comparisons of Various Experimental Methods for Studying Spray Penetration. SAE710571
17. J. Arregle, V. Pastor and S. Ruiz. The Influence of Injection Parameters on Diesel Spray Characterization. SAE1999-01-0200
18. C. Badock, R. Wirth and C. Tropea. The influence of Hydro Grinding on Cavitation Inside a Diesel Injection Nozzle and Primary Break-up under Unsteady Pressure Conditions. Proc. 15th ILASS-Europe 99. Toulouse July 1999.
19. A.J. Yule and D.G. Salters. On the Distance Required to Atomize Diesel Sprays Injected From Orifice-Type Nozzles. Journal of Automobile Engineering, Proc IMechE Vol 209
20. R.E. Morgan, D.A. Kennaird, M.R. Heikal and F. Bar. Characterisation of a High Pressure Diesel Fuel Spray at Elevated Pressures. THIESEL 2000, Valencia 13-15 September 2000.
21. D.A. Kennaird, C. Crua, M.R. Heikal, R.E. Morgan, F. Bar and S.M. Sapsford. A New High Pressure Diesel Spray Research Facility. International Conference on Computational and Experimental Methods in Reciprocating Engines, 1-2 November 2000.C587/040/2000
22. R. Morgan, J. Wray, D.A. Kennaird, C. Crua and M.R. Heikal "The Influence of Injector Parameters on the Formation and Break-Up of a Diesel Spray," SAE paper 2001-01-0529
23. U. Flaid, W. Polach and G. Ziegler. Common Rail Systems (CR-Systems) for Passenger Car DI Diesel Engines; Experiences with Applications for Series Production Projects. SAE1999-01-0191.
24. A.J. Yule, D.G. Salters. On the Distance Required to Atomize Diesel Sprays Injected From Orifice-Type Nozzles. Journal of Automobile Engineering, Proc. Instn. Mech. Engrs. Vol. 209.
25. M. Mouquallid, D. Lisiecki, M. Ledoux, A. Belghit. Study of High Pressure Diesel Sprays. 14th ILASS-Europe 1998

26. B. Jawad, E. Gulari and N.A. Henein. Characteristics of Intermittent Fuel Sprays. Combustion and Flame 1992.
27. C. Heimgärtner and A. Leipertz. Investigation of the Primary Spray Breakup Close to the Nozzle of a Common – Rail High Pressure Diesel Injection System. SAE 2000-01-1799
28. K.R. Browne, I.M. Partridge, and G. Greeves. Fuel property Effects on Fuel/Air Mixing in an Experimental Diesel Engine. SAE 860223.

DEFINITIONS

S	Fuel spray penetration
ΔP	Pressure difference across nozzle
$\mathbf{T_a}$	Atmospheric pressure